A STOCHASTIC TREATMENT OF ROPE STRENGTH PREDICTION

By Hwai-Chung Wu, John F. Mandell
and Stanley Backer

MITSG 90-19

Sea Grant College Program
Massachusetts Institute of Technology
Cambridge, Massachusetts 02139

Grant No: NA86AA-D-SG089
Project No: RT-11

ABSTRACT

This study is concerned with the static tensile performance of braided ropes. Statistical theories are applied to determine the most probable rope strength. In addition to the structural modelling, the failure strain distribution of individual rope components is also included. Extremes of no-friction and infinite-friction (no relative movement) conditions are considered. A Monte Carlo technique and probability model are used in the former case where no load transfer is considered around failed strands. In the latter case, a failure probability analysis is developed based on a proposed local load-sharing rule. Experimental results agree well with the predictions for small nylon and polyester double-braided ropes. Such a statistical approach also provides a promising method for estimating the effects of local wear/abrasion damage on subsequent performance.

Contents

1 Introduction

The theoretical strength of materials, which may be approximated as 10 % of the elastic modulus by considering the atomic bonding [13], is usually much higher than actual observed values. This discrepancy was first ascribed to the presence of flaws [7]. The position and strength distribution of such flaws are, in general, random occurrences. Thus, the event of the failure can be modelled as a stochastic process and will be approached here based on statistical analysis.

The common (though incorrect) practice is to assume that the strength of a simple bundle of parallel filaments is equal to the average strength manifested by individual filaments when tested separately, failing due to its stochastic nature. As pointed out by Coleman [3] the ratio of the tensile strength of a bundle to the mean tensile strength of the constituent filaments decreases monotonically with increasing dispersion (i.e. coefficient of variation) in the strength of the constituent filaments. In general, the tensile strength of a large bundle has the same order of magnitude, but is less than the mean strength of the component filaments [3].

Many successful statistical theories have been proposed in the literature to describe fracture phenomena in metals, textiles, and other materials. Peirce [15] was among the first to investigate the relationship between specimen length and its strength, from which followed the weakest-link theory, i.e. that the strength of a test specimen is that of its weakest element of length. The tensile strength thus decreases with increasing length of the specimen in a way which is definitively calculated from the distribution of strength of shorter specimens. By a similar approach, Weibull [29] proposed a useful distribution function as

$$F(x) = 1 - e^{-(\frac{x}{x_0})^m} \qquad (1)$$

where x_0 and m are material constants. The Weibull distribution, in which the weakest-link concept is implicitly considered, is more tractable than the normal distribution (assumed by Peirce).

A more general aspect of statistical models applicable to the prediction of material strength was discussed by Epstein [5]. Daniels [4] and Gücer et al [8] later developed statistical models for the strength of bundles of fibers. In particular, Gücer suggested that a second fracture mode exists, which is not controlled by the weakest element if the elements fracture independently. Zweben and Rosen [25,31,32] further applied the chain-of-bundles theory to study composite strength. They successfully demonstrated that the composite failure is associated with the accumulation of many fiber breaks. In their study, the matrix is considered to be purely a medium for the transmission of shear stress between the fibers. The load concentration caused by fiber breaks was later accounted for in their theory to improve agreement with experimental data [32].

More recently, Phoenix and co-workers [9,10,16,21,28] reported on a series of studies based on the chain-of-bundles probability model. Their treatment is more general in terms of statistics, as related to fiber/matrix composites and fibrous bundles such as yarns and cables. The load-sharing rules after fiber breaks occur were extensively explored. Shahpurwala and Schwartz [27] attempted to predict the tensile strength of woven fabrics when the strength distributions of the constituent yarns were known. They adopted Daniels' approach [4], in which the fabric was considered as a loose bundle of yarns, with no yarn interactions.

Beyond the ideal geometry of perfectly parallel elements, Phoenix and Taylor [20] and Phoenix [18] considered the effect of slackness on the bundle strength distribution by introducing a second random variable of individual length l. This slack effect turned out to be very important when twisted fiber bundles (such as yarns and cables) are considered [19].

It is important to note that all of the above theories were limited to elastic materials, where in particular, material strength is independent of the loading rate. Therefore, attempts to calculate the tensile strength distribution of a structure (i.e.

generalized bundle) from a given probabilisitic di ·ribution of the constituents are meaningful in light of the above referenced reports.

In this study, statistical approaches are applied to predict the tensile behavior of small synthetic fiber ropes. The ropes of interest are double-braided, composed of two separable layers, i.e. sheath and core (see Figure 1). In general, the fibers within the same layer are (by specification) identical. However, different materials may be used in either layer. In the current study, the same generic yarn type was used in the sheath and core layers, but in different deniers.

2 Statistical Strength of Ropes

In the context of common bundle theory, rope can be considered as a bundle of strands. A strand (or yarn) is here regarded as a unit element, instead of a fiber in the previous case. At first, no friction or interaction between strands is assumed (hence no load sharing whatsoever); other frictional constraints will be considered later. The geometry of the individual strand is described as a helix with a sinusoidal undulation in radial direction [12,1,26]. The primary effect of the helical geometry on the behavior of the parallel element model is to alter the local element strain with respect to the axial rope strain. In the structural models of ropes [12,26,30], assumed geometries of rope strands before and after stretching can then be used to calculate local length difference (hence local strand strain). In this manner, a local strain distribution is determined with respect to an axial rope strain. The total rope rupture occurs when a local maximum strain reaches its failure value. This paper follows an approach similar to that of Phoenix [19].

Let $X_{ij}(\epsilon_r)$ be the component of the tensile force of element ij in the direction of the rope axis at an axial rope strain of ϵ_r. Where the ijth element is the jth element in layer i. Since there are only two layers in a double-braided rope, i runs from 1 to

2. Also, ξ_{ij}'s are identically independent random variables representing the breaking strain of the ijth element with the cumulative density function (c.d.f.), $F(\epsilon)$.

Consider the load-strain relationship of element ij to be

$$Y_{ij}(\epsilon_{ij}) = \begin{cases} 0 & \text{for} \quad \epsilon_{ij} < 0 \\ q_{ij}(\epsilon_{ij}) & \text{for} \quad 0 < \epsilon_{ij} < \xi_{ij} \\ 0 & \text{for} \quad \xi_{ij} < \epsilon_{ij} \end{cases}$$

where Y_{ij} : the range of tensile force on the element ij

ϵ_{ij} : the local strain of the element ij

q_{ij} : the finite positive value of tension in element ij

Here the element can only support a load in tension, and it carries no load after it breaks. Thus,

$$X_{ij}(\epsilon_{ij}) = \begin{cases} 0 & \text{for} \quad \epsilon_{ij}(\epsilon_r) < 0 \\ q_{ij}[\epsilon_{ij}(\epsilon_r)] \cos\alpha_{ij} & \text{for} \quad 0 < \epsilon_{ij}(\epsilon_r) < \xi_{ij} \\ 0 & \text{for} \quad \xi_{ij} < \epsilon_{ij}(\epsilon_r) \end{cases} \tag{2}$$

where α_{ij} = local helix angle of the jth element in layer i.

Therefore, the rope load at rope strain ϵ_r, $Q_n(\epsilon_r)$, is the sum of the element forces X_{ij}:

$$Q_n(\epsilon_r) = \sum_{i=1}\sum_{j=1} X_{ij}(\epsilon_r) \tag{3}$$

That is, the rope strength Q_n^*, is the maximum load achieved as the rope strain is increased.

The actual local load distribution of individual strands (prior to first strand failure) depends on the frictional constraints imposed by the surrounding material. Two extreme conditions, i.e. zero friction and infinite friction, are considered as follows. In the former case, no load sharing after initial strand failure is required; it can be analyzed by the Monte Carlo technique or the maximum strength analysis. In the latter case, a local-load sharing rule was developed to account for the local force concentration, and a failure probability model was established.

2.1 Monte Carlo simulation

In brief, Monte-Carlo simulation is a stochastic-process simulation (also called discrete-event simulation) [6]. It refers to the use of mathematical models to study systems that are characterized by the occurrence of discrete, random events. These individual events are represented by random variables whose values are generated by a computer. The randomness that is encountered in a real system can thereby be synthesized, allowing the behavior of the original system to be reproduced artificially. Such studies allow assessment of the expected behavior of the system.

For the rope problem, the main procedure is to simulate the outcomes of Q_n^*. To achieve this, the first step is to generate the random variables (rupture strains), ξ_{ij}'s, that are governed by a Weibull density function. The inverse transformation method offers a simple and straightforward approach to the generation of the required nonuniform random variate, ξ_{ij}.

For each simulation run, n random numbers between 0 and 1, U_{ij}'s, were generated using a computerized random-number generator. Then the n numerical values for the failure strains of the elements were obtained by the following formula [19]

$$\xi_{ij} = \epsilon_0[\ln(\frac{1}{1-U_{ij}})]^{\frac{1}{r}}$$

where ϵ_0 and r are the scale and shape parameters of Weibull function of the failure strains for the strands. The second step is to compute the rope load, Q_n, from equations 2 and 3, and then Q_n^* is given by the maximum value, i.e. rope strength. Repeating the steps, enough outcomes are generated for Q_n^* to estimate the expected performance measures of strength, mean and standard deviation.

2.2 Maximum strength analysis

Apart from the simulation, there is a second approach which can be used to estimate the strength of ropes. This analysis was originally proposed by Platt et al [22,23,24] to study the translation of mechanical properties of fibers into yarns and strands. The following conditions are assumed in this study:

1. The load-strain curves are identical for individual strands until failure.
2. The failure strains follow a definite distribution, $F(\epsilon_{ij})$, such as Weibull type.
3. No interaction (hence no friction) occurs between strands.
4. Rope load is equally carried by each unfailed strand.

For a given rope strain, the actual strain along the rope strand can be calculated [30]. The relationship is obtained based on the assumed geometry. The rope load equals the summation of force components along rope axis over all strands. Therefore,

$$Q_n(\epsilon_r) = N_s\overline{Q}[\epsilon_{ij}(\epsilon_r)]$$

where $Q_n(\epsilon_r)$: rope load at a rope strain ϵ_r

$\overline{Q}$: average strand force along rope axis at a rope strain ϵ_r

$\epsilon_{ij}(\epsilon_r)$: actual strain of the j-th strand in layer i at a rope strain ϵ_r

N : total number of rope strands

N_s : number of survival strands at a rope strain ϵ_r

Since the failure probability $F(\epsilon)$ is known (see equation 5)

$$N_s = N(1 - F(\epsilon)) \qquad \text{and} \qquad Q_n(\epsilon_r) = N(1 - F(\epsilon_{ij}))\overline{Q}$$

The rope strength is the maximum value Q_n can achieve. Hence, the solution of $\frac{dQ_n}{d\epsilon_r} = 0$ yields the maximum value and the corresponding rope strain at failure.

For a double-braided rope, $\overline{Q}$ can be expressed as:

$$\overline{Q}_i = \frac{\sum\limits_{j=1} X_{ij}}{N_i} \qquad\qquad i = 1,2$$

where X_{ij} = defined in equation 2

N_i = total number of rope strands in layer i

$$\text{Thus. } Q_n(\epsilon_r) = (1 - F_1(\epsilon_r)) \sum_{j=1} X_{1j} + (1 - F_2(\epsilon_r)) \sum_{j=1} X_{2j} \tag{4}$$

where $F_{1,2}(\epsilon_r)$ = failure probability of strands in layers 1 and 2 at a rope strain ϵ_r.

Since there is no mathematical closed form solution for Q_n, it is difficult to calculate its first derivative. However, the maximum value of Q_n can be found by a numerical technique.

2.3 Failure probability analysis

In order to explore the frictional effect on rope strength, a local stress concentration around a broken element must be considered, i.e. a local-load sharing rule should be implemented.

For a given rope strain, the local strand strain can be calculated based on the assumed geometry, such as in the infinite friction case [30]. Then the survival probability of each strand is determined from the failure strain-probability curves. The total survival probability of this strand assembly should be the summation of all possible survival modes except the one in which all strands fail.

$$P_{tot} = \sum_{i=0}^{n-1} P_i$$

$$\text{and} \quad P_i = \begin{cases} S_1(\epsilon_r)S_2(\epsilon_r)\cdots S_n(\epsilon_r) & i = 0 \\ F_1(\epsilon_r)\cdots F_i(\epsilon_r)S_{i+1}(\epsilon_r)\cdots S_n(\epsilon_r) & i \neq 0 \end{cases}$$

where P_i : survival probability of i strands failed and $(n-i)$ strand survived.

$S_i(\epsilon_r)$: survival probability of strand i at a given rope strain ϵ_r.

$F_i(\epsilon_r)$: failure probability of strand i at a given rope strain ϵ_r.

$= 1 - S_i(\epsilon_r)$

n : total number of strands

The total survival probability is the counterpart of the total failure probability, i.e.

$$P_{tot} = 1 - F_1 F_2 \cdots F_n$$

It is worth noting that the load redistribution around a broken element is taken into account for calculating the survival probabilities of the neighboring elements. The rules are:

1. The first break will take place in the highest strain location.

2. The subsequent breaks will happen in the next highest strain locations after the first break.

3. After the first strand fails (designated A in Figure 2), the load originally carried by the failed strand will be totally transferred to the neighboring parallel strand (B in Figure 2).

4. After both parallel strands fail, they snap back and are stopped by the next cross-over strands, which transfer the load to the surrounding parallel strands equally (C,D,E,F in Figure 2).

3 Results

Specimens of strands were carefully removed from ropes and tested as described earlier [30]. The Weibull distributions of failure strains were obtained as follows (gauge length of 12 in) and plotted in Figure 3

$$F(\epsilon) = 1 - \exp[-(\frac{\epsilon}{.144})^{24.48}] \qquad \text{for PET yarn} \qquad (5)$$
$$F(\epsilon) = 1 - \exp[-(\frac{\epsilon}{.246})^{19.64}] \qquad \text{for nylon yarn}$$

Rope tensile tests were conducted on an Instron servo hydraulic machine in the laboratory. Eye splices were used to properly mount 2 ft rope specimens on the machine. The rope was then subjected to 10 cycles of from 0 to 5% of the breaking strength at a frequency of .05 Hz. Immediately following the last cycle, the rope was loaded to failure at a load rate setting of 30 lbs per second under load control mode.

3.1 Monte Carlo simulation

Figure 4 shows the typical curve of Q_n vs. ϵ_r, where the load drops indicate the occurrence of strand breakage of either layer. Since the core and sheath layers of a double-braided rope are independently considered, two maxima are observed corresponding to the failure of each layer. The rope strength Q_n^* is indicated by the peak value. One hundred and sixty simulations were performed for each type of rope. The cumulative distribution curves of rope strength Q_n^* are plotted in Figure 5.

It should be noted that the load Q_n versus rope strain ϵ_r curves of Figure 4 are determined for the combined sheath and core braids. Determination of loads in the sheath strands is based on the assumption that the core strand is in place, preventing collapse of the sheath. It should be emphasized that this simulation treatment excludes load transfer and thus assumes that sheath and core layers act independently of each other. Obviously where sheath and core interact, the first load peak which occurs in Figure 4 will likely be followed by total rupture of the rope.

3.2 Maximum strength analysis

Q_n vs. ϵ_r is plotted in Figure 6. The strengths of nylon and PET ropes are determined to be 2161 lbs and 2377 lbs respectively. The corresponding failure strains are .276 and .153 for nylon and PET. These predictions (as per Platt) and the results of the previous Monte Carlo simulation are summarized in Table 1. The experimental data and the prediction of the structural modelling [30] without considering the distribution of failure strain of individual strands are also shown with agreements to 10 and 15%. Far better predictions are obtained by considering variation in the strengths of individual strands (or yarns) and the strength/strain values based on the statistical models are seen to be within a few per cent of the experimental values.

3.3 Failure probability analysis

The cumulative failure probability equals $1 - P_{\text{tot}}$. This is plotted in Figures 7 and 8 for PET and nylon ropes respectively. For comparison, the predictions of no-load transfer case with zero friction constraints are also included in the same figures, as well as the corresponding failure density functions. The modes are good indications of the rope failure strains. Similarly, the probability can be plotted against rope load. Again, the rope strength can be obtained from the most probable value. The results are summarized in Table 2.

4 Discussion

4.1 Comparison of different approaches

As discussed in References [12,26,30], the structural modelling approach provides the basis to investigate the behavior of ropes. Different frictional conditions are considered. In general, the trends agree for both nylon and polyester ropes. In addition, the stochastic nature of the failure strength of individual elements is also taken into account by the statistical analysis. In this study, the load-strain curves of individual strands follows a common curve truncated at different positions for different strengths.

For the infinite friction case, the consequences of the strength variation of individual strands are expected not to be significant because that weak flaws are not likely to be located at the highest strain areas. However, on the other hand, the variation is expected to play a more important role in the no friction case. This is due to a averaging effect so that weak flaws can greatly reduce the rope strengths. Indeed, as shown in Table 1 for the no friction case, much better agreements with experimental data are found when statistics are considered.

4.2 Local damage effect

The statistical distribution of strand strength (or failure strain) was obtained from a series of tests on virgin materials. It is quite reasonable to assume a uniform flaw distribution along the strand axis, since the manufacturing process is uniform and continuous. However, the uniformity is violated after the material is employed in service. For example, marine ropes may be subjected to a very severe environmental conditions. A certain portion of the rope strand is directly exposed to the environment. Therefore, a more progressive damage could be developed, such as photodegradation or abrasion. Even inside the rope, internal abrasion can also result in serious damage. In general, such local damage is unavoidable and reduces the performance of ropes [2]. In order to take this effect into account, the distribution of failure strengths (or strains) should be properly expanded. The distribution tests should include several partially damaged strands to study the effects on the final performance.

4.2.1 Reduced failure strain distribution

Consider a failure strain distribution of rope strands after being deployed in service for a period of time. As reported by Hsu [12] and Backer [2] in a pathological study of double-braided ropes (Puget Sound Ropes), only 50-60 % of the new yarn strength was found. Based on this information, new failure strain distributions as shown in Figure 9 can be generated. For case 1, a 60 % retention is assumed (i.e. the initial value of the failure strain of the new rope in Figure 9a is reduced from .18 to .11), but the ultimate failure strain (.27) is unchanged. Then, the scale and shape parameters of a Weibull distribution are found to satisfy the above conditions. In case 2, the same shape parameter of the original distribution is used, but the scale parameter is scaled down 60%.

The rope strength predictions from this failure probability analysis are now plotted in Figures 10 and 11 for the infinite friction and for the zero friction (no load sharing) cases respectively. For case 1, the rope strength is calculated to remain 60 % of the original value; while a 40 % retention is expected for case 2. It is noted that a much wider range of failure strengths is present for the first case. It should be also pointed out here that the residual strengths of Puget Sound ropes were reported to be 50-60 % of the new rope strengths (similar range to that of the yarns) [12]. Our predictions for the first case agree with their results.

5 Conclusions

In this study, statistical theory was applied to predict the tensile behavior of small double-braided ropes. Structural modelling has also been undertaken without superposition of statistics.

Two cases are considered, one with no friction between strands, the other with infinite friction. For the no friction case, rupture strains are randomly assigned to all rope strands based on the experimentally determined strand rupture-strain distribution. The computed strain distribution for each given rope strain is then compared to the randomly assigned rupture strains so as to identify the occurrence of strand failure. Then the rope strain is increased, and the procedure is repeated until the maximum rope strength is reached. A second analysis after Platt is also successfully developed. In this analysis, the average survival probability of strands is determined, then the total number of survival strands is multiplied by the average load per strand to calculate the total rope loads. Both approaches provide very good predictions to the experimental results.

For the infinite friction case, failure probability distribution versus strain is determined experimentally for strands, thus permitting conversion of local strain distribution within the stretched rope to the total failure probability distribution of the strand assembly (rope). Therefore, the total failure probability versus rope load can then be generated. Rope strength is thus indicated by the most probable value of this failure probability distribution.

Furthermore, these proposed approaches can also be used to study local damage effects on the final performance of ropes. The local wear/abrasion damage is generally unavoidable and difficult to consider quantitatively. The strength reduction is strongly dependent of the severity of local damage; the damage can be included through the appropriate study of rupture-strain distribution of individual strands.

References

[1] Backer, S. and Hsu, P., "Structures with Partial Frictional Constraints", Proceedings of the Third Japan-Australia Joint Symposium on Objective Measurement: Applications to Product Design and Process Control, Kyoto, Japan, September 5-7, 1985, p101.

[2] Backer, S. and Seo, M. H., "Mechanics of Degradation in Marine Rope", Proceedings of the Third Japan-Australia Joint Symposium on Objective Measurement: Applications to Product Design and Process Control, Kyoto, Japan, September 5-7, 1985, p653.

[3] Coleman, B. D., "On the Strength of Classical Fibers and Fiber Bundles", *J. Mech. Phys. Solids, Vol. 7*, p60 (1958).

[4] Daniels, H. E., "The Statistical Theory of the Strength of Bundles of Threads" *Proc. Roy. Soc. A183*, p405 (1944).

[5] Epstein, B., "Statistical Aspects of Fracture Problems", *Appl. Phys. Vol 19*, p140 (1948).

[6] Gottfried, Byron S., "Elements of Stochastic Process Simulation", Prentice-Hall, 1984.

[7] Griffith, A. A., "The Phenomena of Rupture and Flow in Solids", *Phil. Trans. Roy. Soc. 221A*, p163 (1920).

[8] Gũcer, D. E., and Gurland, J., "Comparison of the Statistics of Two Fracture Models", *J. Mech. Phys. Solids, Vol. 10*, p365 (1962).

[9] Harlow, D. G., and Phoenix, S. L., "The Chain-of-bundles Probability Model for the Strength of Fibrous Materials I: Analysis and Conjectures", *J. Composite Materials 12*, p196 (1978).

[10] Harlow, D. G., and Phoenix, S. L., "The Chain-of-bundles Probability Model for the Strength of Fibrous Materials II: A Numerical Study of Convergence", *J. Composite Materials 12*, p314 (1978).

[11] Harlow, D. G., and Phoenix, S. L., "Probability Distribution for the Strength of Composite Materials I: Two-level Bounds", *Int. J. Fracture, Vol. 17*, p347 (1981).

[12] Hsu, P., "Fracture Mechanisms of Synthetic Fiber Ropes", Ph.D. Thesis, The Department of Mechanical Engineering, Massachusetts Institute of Technology (1984).

[13] Kanninen, M. F., and C. H. Popelar, "Advanced Fracture Mechanics", Oxford University Press, New York, 1985.

[14] Karlin, S., "A First Course in Stochastic Processes", Academic Press, New York, 1968.

[15] Peirce, F. T., "Tensile Tests for Cotton Yarns v. - 'The weakest link' - Theorems on the Strength of Long and of Composite Specimens" *J. Text. Inst. 17*, p355 (1926).

[16] Phoenix, S. L., "Probabilistic Concepts in Modeling the Tensile Strength Behavior of Fiber Bundles and Unidirectional Fiber/Matrix Composites", *Composite Materials: Testing and Design (Third Conference), ASTM, STP546*, p130 (1974).

[17] Phoenix, S. L., "Statistical Analysis of Flaw Strength Spectra of High-modulus Fibers", *Composite Reliability, ASTM, STP 580*, p77 (1975).

[18] Phoenix, S. L., "Probabilistic Inter-fiber Dependence and the Asymptotic Strength Distribution of Classic Fiber Bundle", *Int. J. Eng. Sci., 13*, p287 (1975).

[19] Phoenix, S. L., "Statistical Theory for the Strangth of Twisted Fiber Bundles with Applications to Yarns and Cables", *Text. Res. J. 49*, p407 (1979).

[20] Phoenix, S. L., and Taylor, H. M., "The Asymptotic Strength Distribution of a General Fiber Bundle", *Adv. Appl. Prob., 5*, p200 (1973).

[21] Pitt, R. E., and Phoenix, S. L., "On Modelling the Statistical Strength of Yarns and Cables under Localized Load-sharing among Fibers", *Text. Res. J. 51*, p408 (1981).

[22] Platt, M. M., Klein, W. G., and Hamburger, W. J., "Mechanics of Elastic Performance of Textile Materials, Part IX", *Text. Res. J., 22*, p641 (1952).

[23] Platt, M. M., Klein, W. G., and Hamburger, W. J., "Mechanics of Elastic Performance of Textile Materials, Supplement to Part IX", *Text. Res. J., 22*, p827 (1952).

[24] Platt, M. M., Klein, W. G., and Hamburger, W. J., "Mechanics of Elastic Performance of Textile Materials, Part XI", *Text. Res. J., 24*, p907 (1954).

[25] Rosen, B. W., "Tensile Failure of Fibrous Composites", *AIAA J. 2*, p1985 (1964).

[26] Seo, M. H., "Mechanical Deterioration of Synthetic Fiber Rope in Marine Environment", Ph.D. Thesis, The Department of Mechanical Engineering, Massachusetts Institute of Technology (1988).

[27] Shahpurwala, A. A., and Schwartz, P., "Modeling Woven Fabric Tensile Strength Using Statistical Bundle Theory", *Text. Res. J. 59*, p26 (1989).

[28] Smith, R. L., and Phoenix, S. L., "Asymptotic Distributions for the Failure of Fibrous Materials under Series-parallel Structure and Equal Load-Sharing", *J. Appl. Mech., Vol. 48*, p75 (1981).

[29] Weibull, W., "A Statistical Distribution Function of Wide Applicability", *J. Appl. Mech. 18*, p293 (1951).

[30] Wu, H.C., "Modelling of Fibrous Assemblies - Tensile and Bending Behavior", Ph.D. Thesis, The Department of Materials Science and Engineering, Massachusetts Institute of Technology (1990).

[31] Zweben, C., "Tensile Failure of Fiber Composits", *AIAA J. 6*, p2325 (1968).

[32] Zweben, C., and Rosen, B. W., "A Statistical Theory of Material Strength with Application to Composite Materials", *J. Mech. Phys. Solids Vol. 18*, p189 (1970).

Table 1: Summary of predictions obtained from different statistical and structural approaches and experiments. No friction.

		PET Rope	Nylon Rope
Experiment[1]	Strength (lb)	2403 (3%)[3]	2235 (1%)
	Strain	.159 (2%)	.283 (1%)
Monte Carlo[2]	Strength (lb)	2480(+3%)[4]	2275 (+2%)
	Strain	.157 (-1%)	.278 (-2%)
Maximum Strength	Strength (lb)	2377 (-1%)	2161 (-3%)
	Strain	.153 (-4%)	.276 (-2%)
Failire Probability	Strength (lb)	2549 (+6%)	2297 (+3%)
	Strain	.156 (-2%)	.270 (-5%)
Structural Modeling	Strength (lb)	2673 (+11%)	2567 (+15%)
	Strain	.170 (+7%)	.300 (+6%)

[1] : average of 5 tests [2] : mean of 160 simulations [3] : coefficient of variation [4] : error compared with exptl.

Table 2: Summary of predictions obtained from different approaches compared to experiments, Infinite friction.

		PET Rope	Nylon Rope
Experiment[1]	Strength (lb)	2403 (3%)[3]	2235 (1%)
	Strain	.159 (2%)	.283 (1%)
Failure Probability[2]	Strength (lb)	2323(−3%)[4]	1907 (-15%)
	Strain	.141 (-11%)	.240 (-15%)
Structural Modeling	Strength (lb)	2297 (-4%)	1938 (-13%)
	Strain	.143 (-10%)	.246 (-13%)

[1] : average of 5 tests [2] : the most probable values. [3] : coefficient of variation [4] : error compared with exptl.

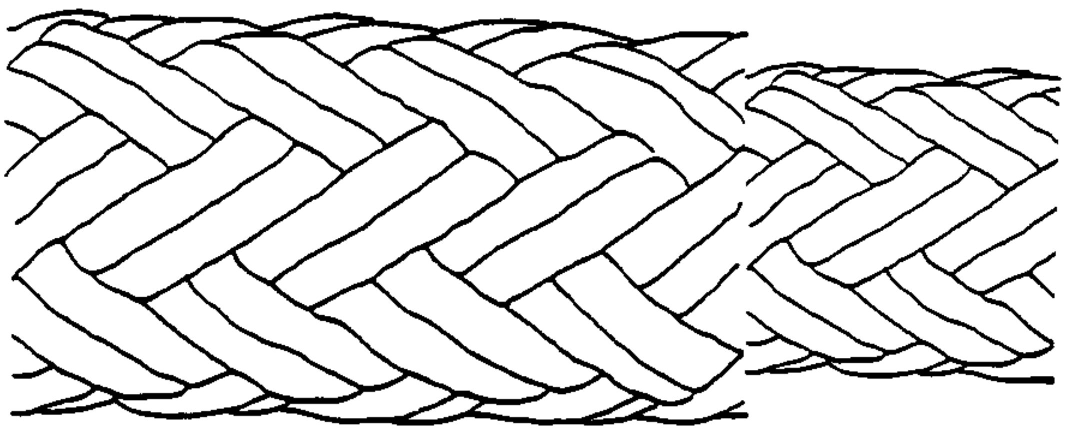

Figure 1: Schematic diagram of double-braided ropes.

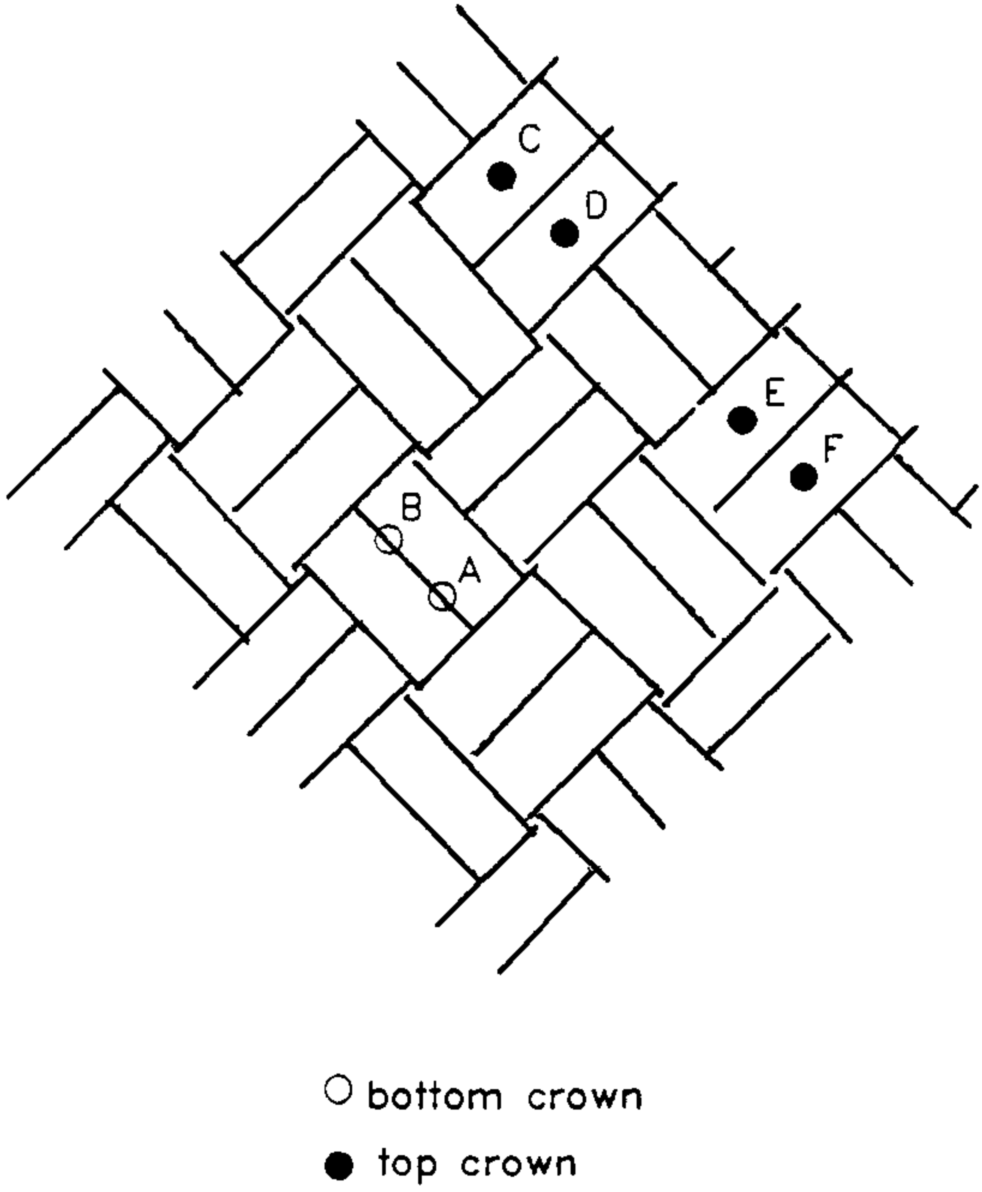

Figure 2: Schematic diagram of rope structure showing local-load transfer, the first break occurs at A.

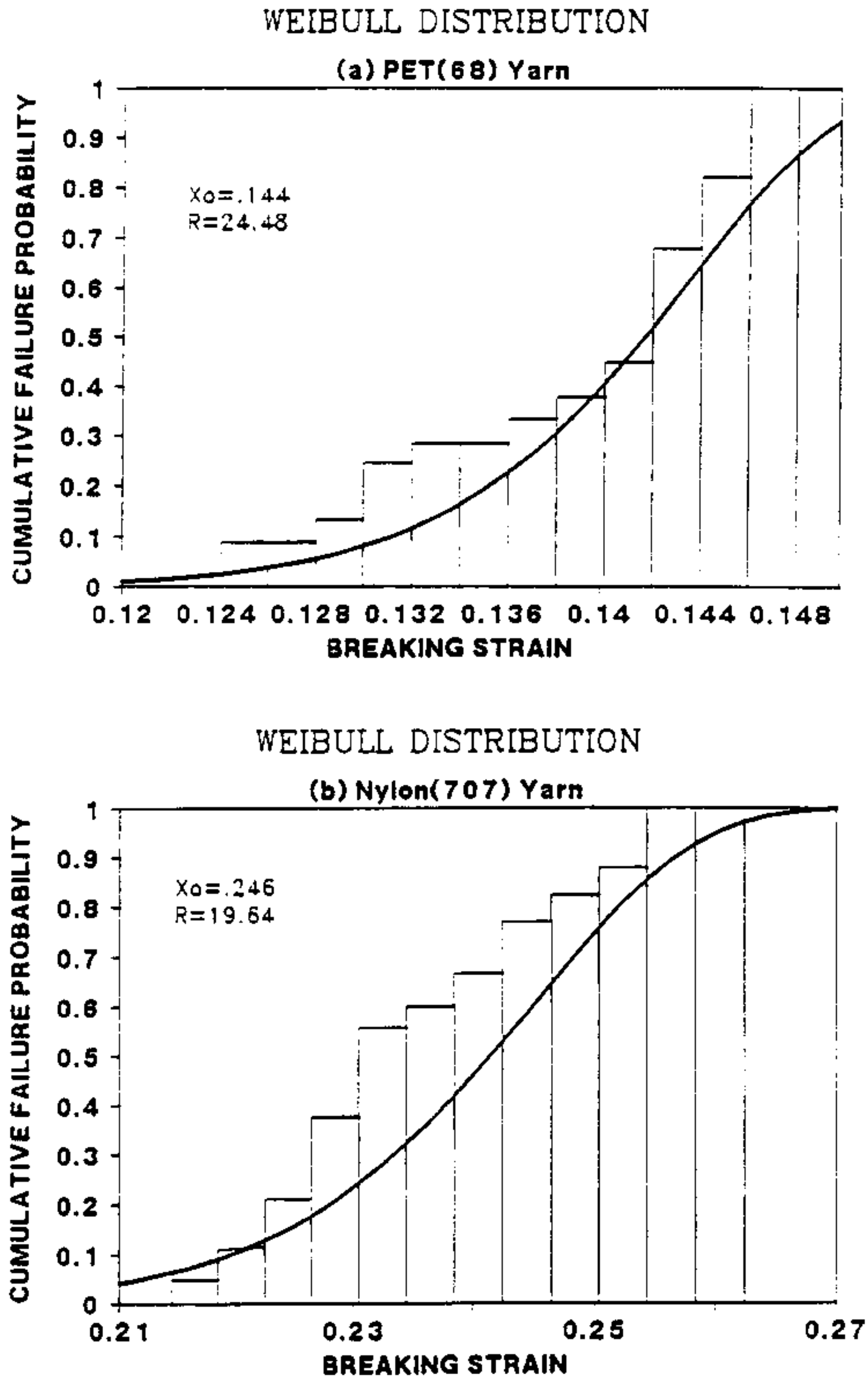

Figure 3: The Weibull distributions of failure strains of rope yarns. (a) PET Yarn (b) nylon Yarn.

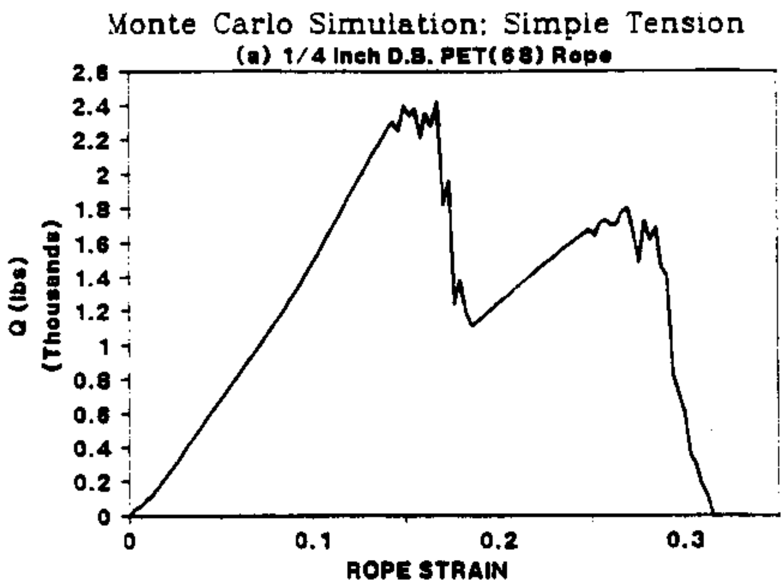

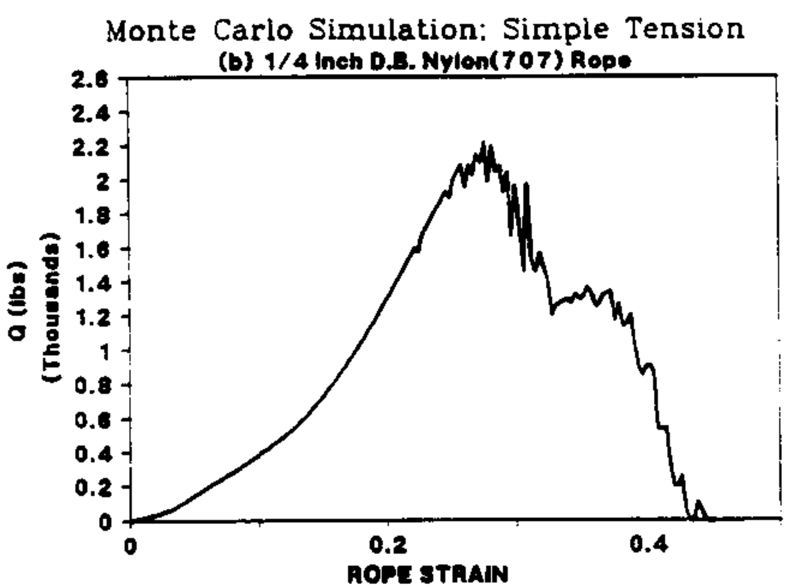

Figure 4: Typical Monte Carlo simulation curves of rope load Q_n vs. rope strain ϵ_r, rope strength is indicated by the highest peak, Tension only. (a) PET (b) nylon.

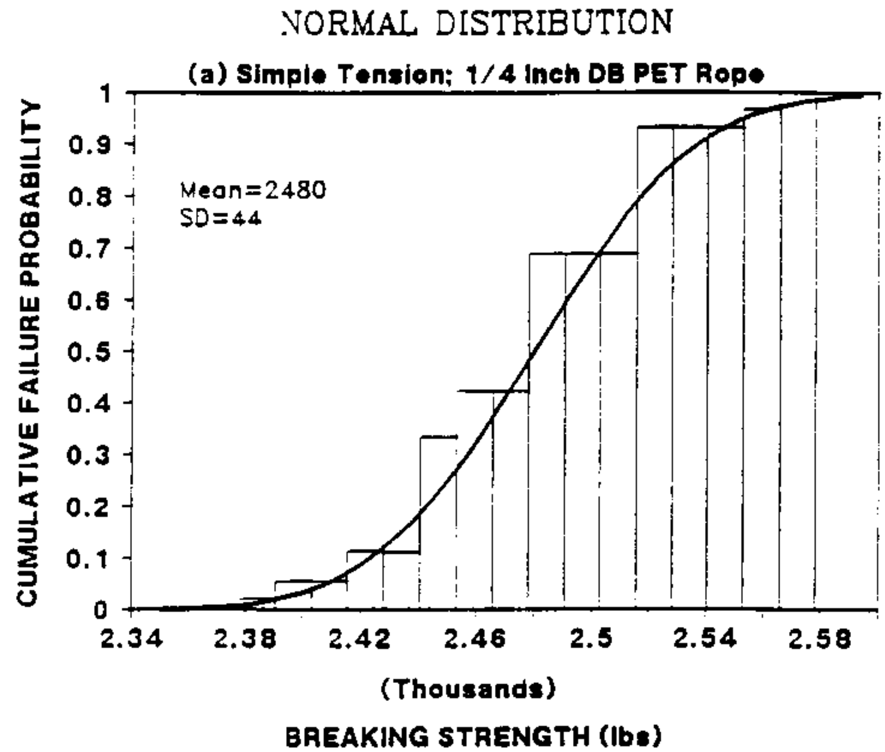

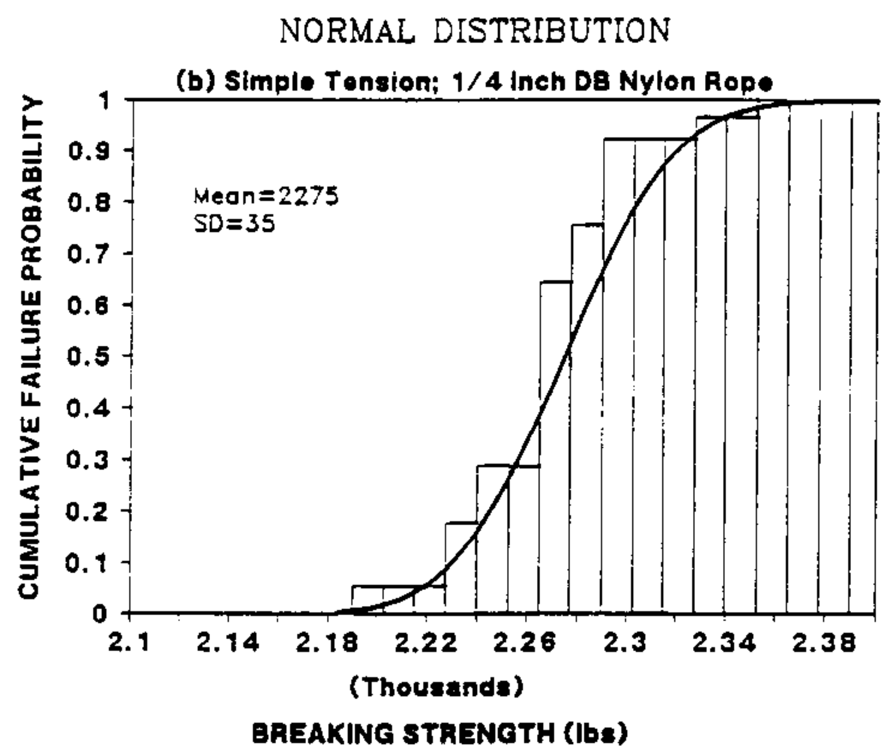

Figure 5: Strength distribution curves of ropes showing mean values of 160 Monte Carlo simulations. (a) PET (b) nylon.

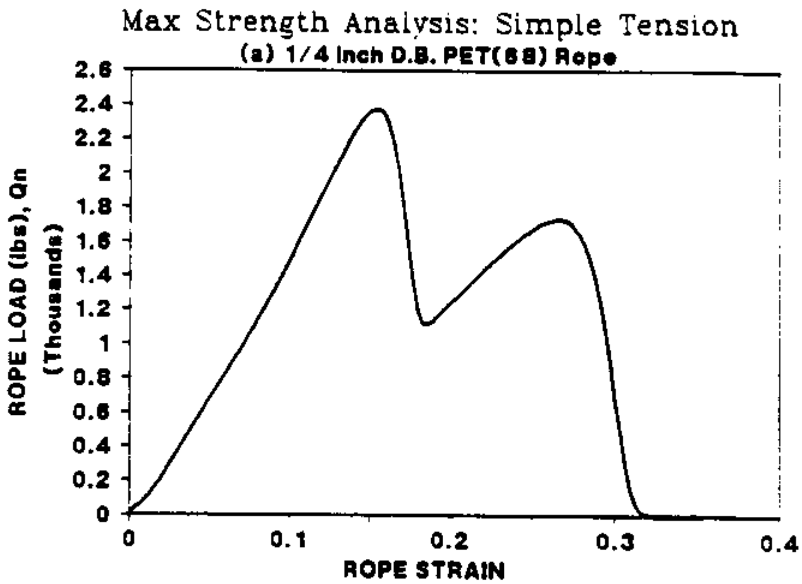

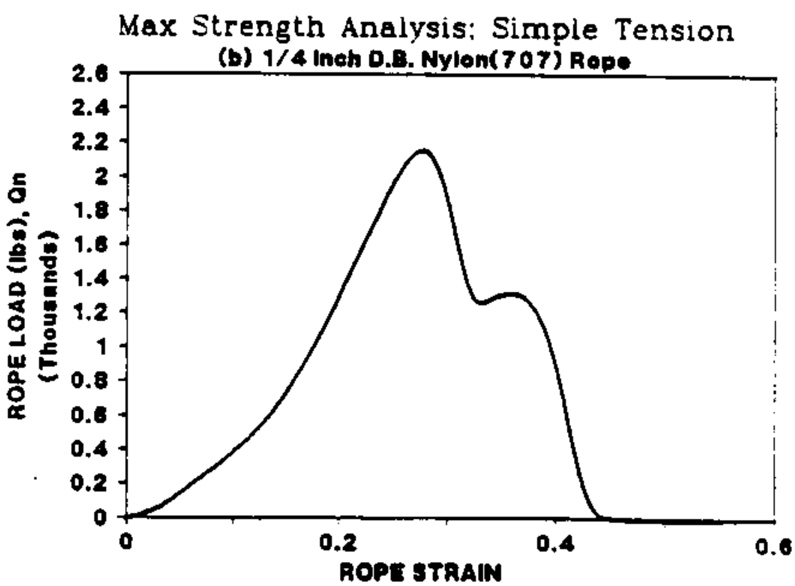

Figure 6: Rope load vs. rope strain obtained from the maximum strength analysis, Tension only. (a) PET (b) Nylon.

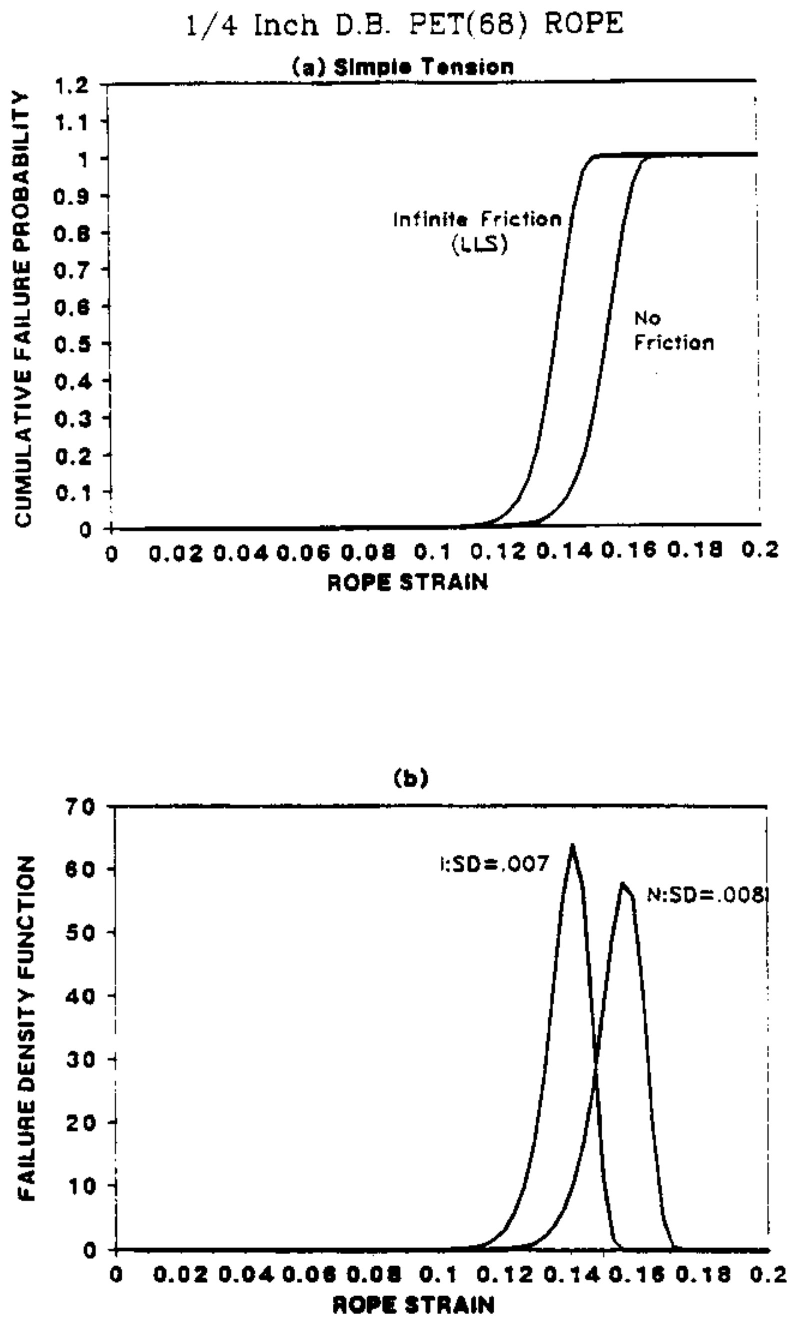

Figure 7: Failure probability vs. rope strain for two friction constraints, Tensile only, PET rope. (a) Cumulative failure probability (b) Failure density function

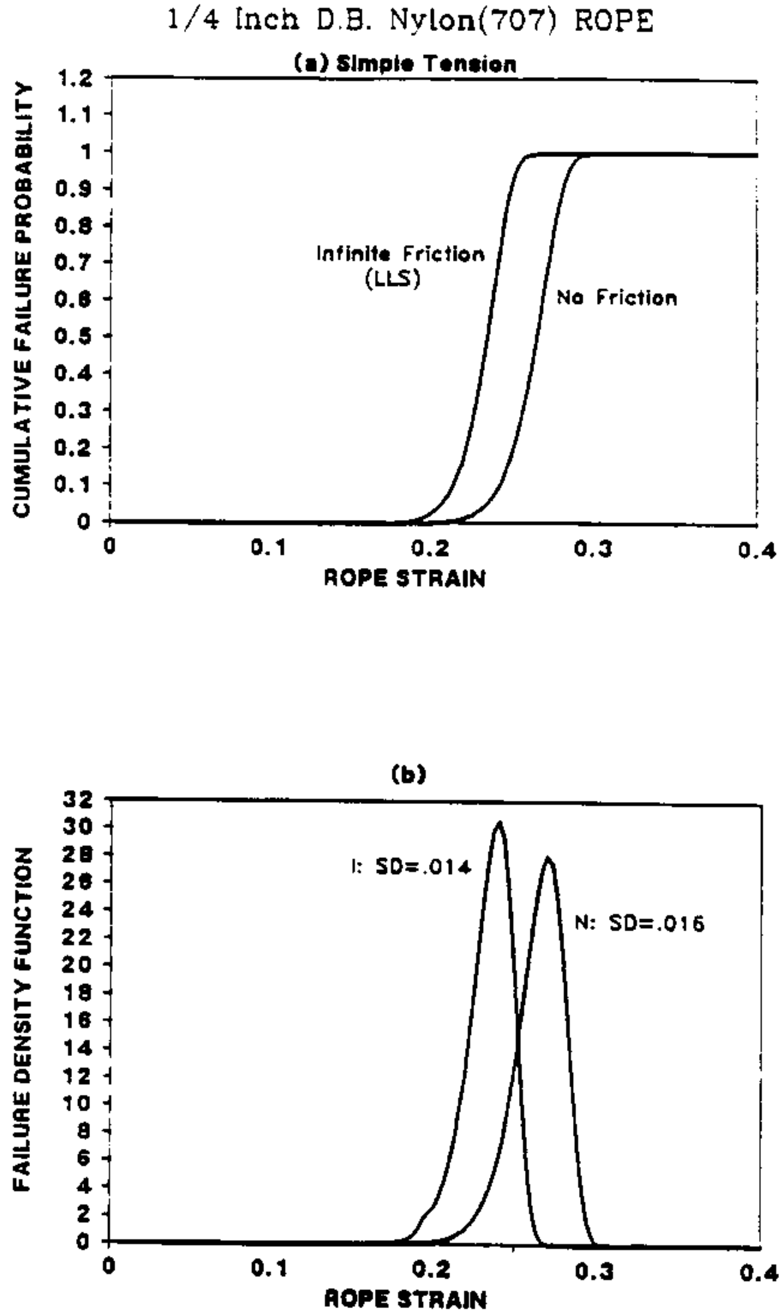

Figure 8: Failure probability vs. rope strain for two friction constraints, Tensile only, Nylon rope. (a) Cumulative failure probability (b) Failure density function

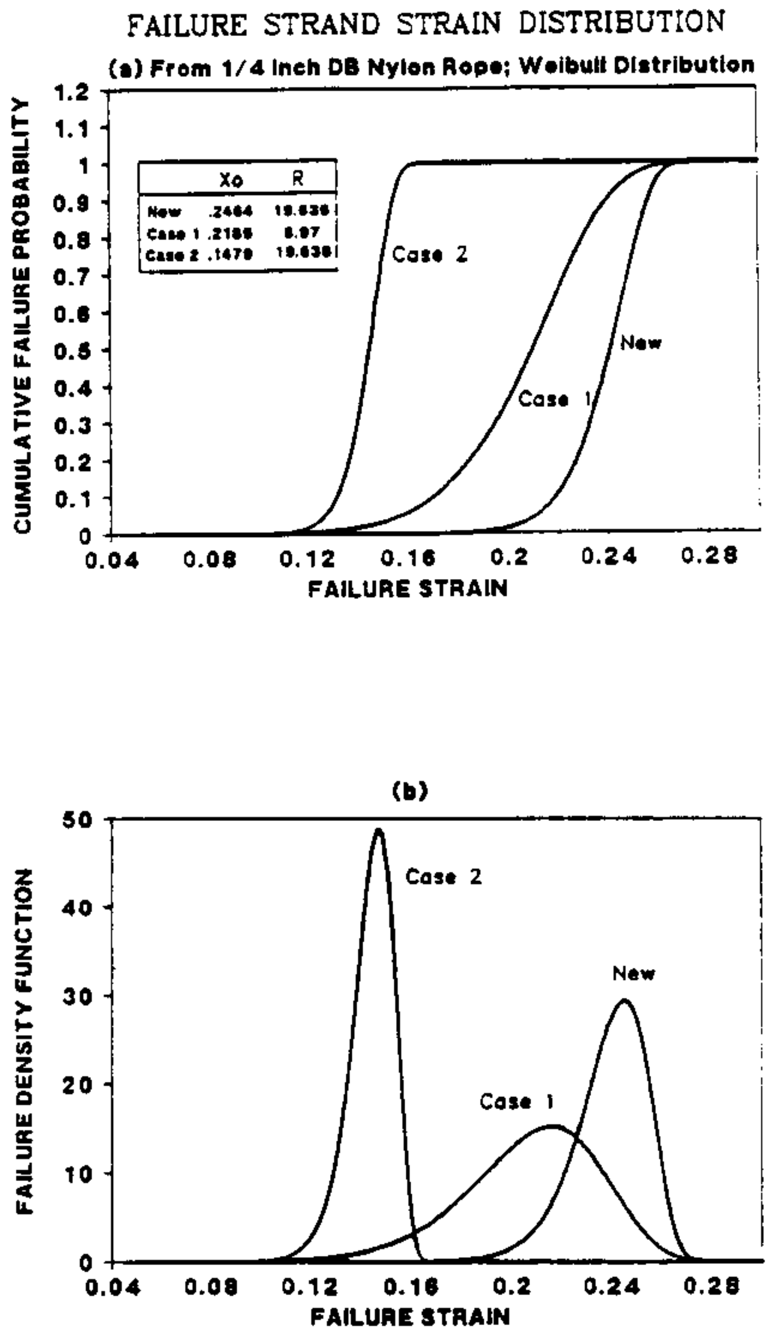

Figure 9: The Weibull Distribution of Failure Strain of Nylon Strand for New and Used Ropes, (a) Cumulative Failure Probability (b) Failure Density Function

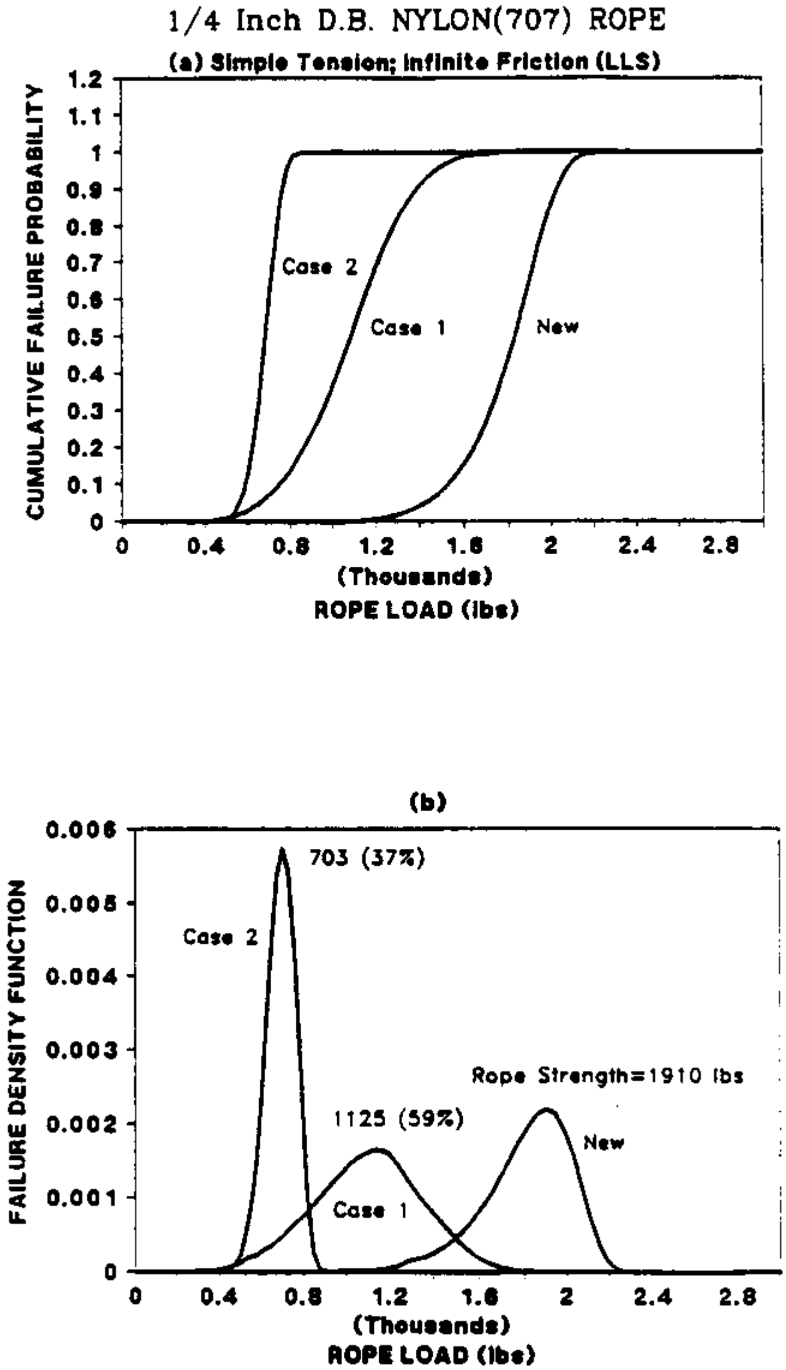

Figure 10: Failure Probability vs. Rope Load for New and Used Nylon Ropes, Infinite Friction(LLS), (a) Cumulative Failure Probability (b) Failure Density Function

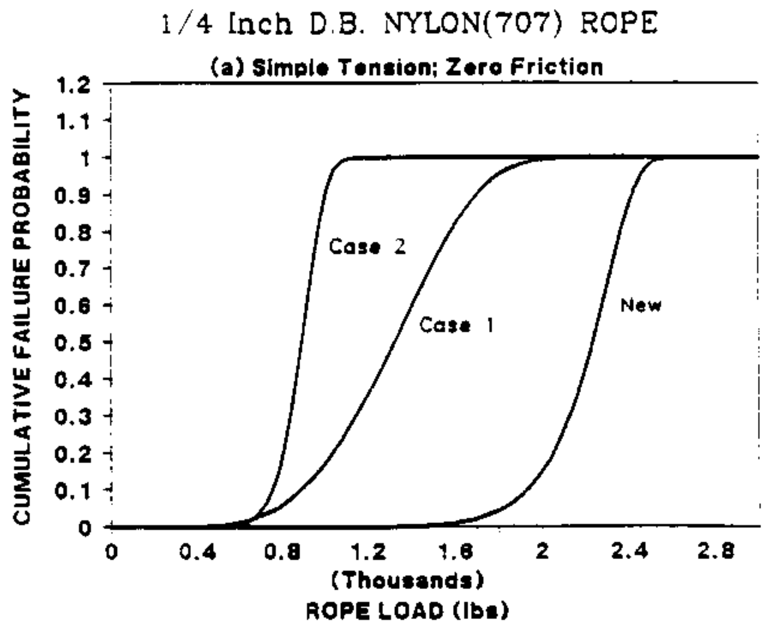

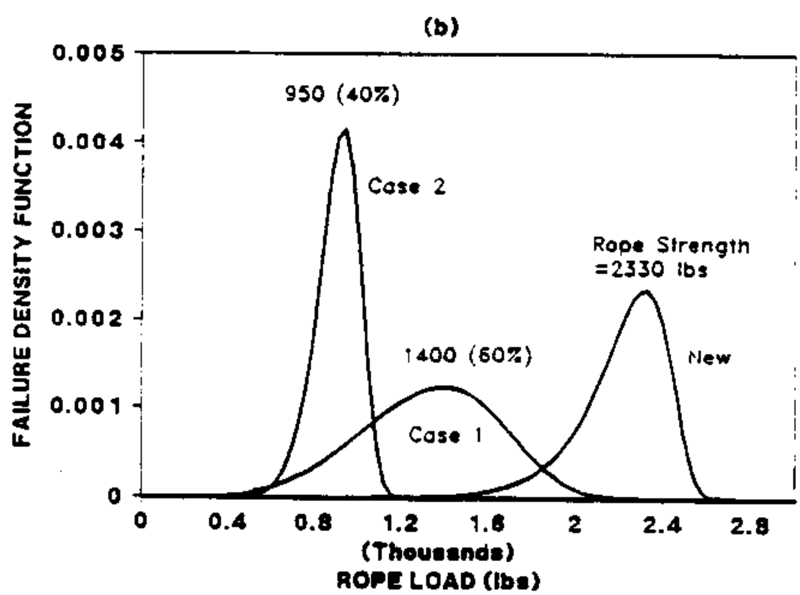

Figure 11: Failure Probability vs. Rope Load for New and Used Nylon Ropes, Zero Friction (No Load Sharing), (a) Cumulative Failure Probability (b) Failure Density Function